

RESEARCH ARTICLE

## The removal of Hexavalent chromium; (Cr (VI)) by ZnO/LECA as a nano photocatalyst using full factorial experimental design

Safoora Karimi <sup>1,2</sup>, Aref Shokri <sup>2,3\*</sup>

<sup>1</sup> Department of Chemical Engineering, Jundi-Shapur University of Technology, Dezful, Iran

<sup>2</sup> Jundi-Shapur research institute, Dezful, Iran

<sup>3</sup> Department of chemistry, Faculty of Science, Payamenoor University, Tehran, Iran.

### ARTICLE INFO

#### Article History:

Received 2021-03-12

Accepted 2021-05-25

Published 2021-08-01

#### Keywords:

Nano photocatalyst

Cr(VI)

ZnO supported on LECA

full factorial

experimental design

### ABSTRACT

In this research, a synthesized nano photocatalyst was prepared by supporting ZnO nanoparticle on Lightweight expanded clay aggregate (LECA). The catalyst was synthesized by co-precipitation method. The SEM, FT-IR and XRD tests were used to characterize ZnO/LECA, which was employed for photocatalytic removal of Cr (VI) from aqueous solution in batch photoreactor. The full factorial experimental design (FFD) was used for the statistical analysis of data. The influence of catalyst amounts, pH, and initial concentration of Cr (VI) was investigated on the reduction of Cr (VI) to Cr (III). The number of active sites was increased with an increase in the concentration of catalyst to some extent. Also, the selection of other factors in optimized amount was important. The optimal conditions were obtained at 0.75 g/l of photocatalyst, pH at 5 and 20 mg/l of Cr(VI). The experimental and predicted reduction efficiency by FFD at optimal conditions were 97.6 and 96.18%, respectively. The comparison of experimental and predicted data showed a good agreement between them.

### How to cite this article

Karimi S., Shokri A. The removal of Hexavalent chromium; (Cr (VI)) by ZnO/LECA as a nano photocatalyst using full factorial experimental design. J. Nanoanalysis., 2021; 8(3): 167-175. DOI: 10.22034/jna.001.

### INTRODUCTION

The Cr (VI) is a poisonous pollutant in various industrial sewages and it has toxic activity in many organisms [1-2]. It is a carcinogenic material in humans. Chromium is generally applied for several industrial purposes, including metal processing, industrial plating, leather and textiles [3-5]. The fate of chromium in the environment is related to its chemistry. The Chromium exists in the wastewater in both Cr(III) and Cr(VI). So, the reduction of Cr(VI) to Cr (III) is highly essential to diminish the toxicity of chromium and hinder its mobility[6-7].

Various methods exist for Cr(VI) removal, including chemical reduction, adsorption in adsorbent materials, ion exchange, reduction of microorganisms and photocatalytic degradation [8-12].

Among the treatment process, the photocatalytic is a suitable method for removal of Cr(VI) in an

aqueous solution. These methods are based on the electron-hole mechanism [13-14]. By radiation, the electrons were transferred from the valence band to the conduction band and the electrons in conduction band and holes in the valence band are formed. The electrons in the conduction layer can reduce the Cr(VI) to Cr(III). The photo catalytic reduction of Cr(VI) can be happened by various semiconductors, including TiO<sub>2</sub>, ZnO, CdS and WO<sub>3</sub>[15].

Some researchers have studied that the properties of Zinc oxide including insolubility in water, high chemical stability, non-toxic and low cost are suitable for the photo catalytic reduction process. Zinc Oxide is a semiconductor with high photocatalytic efficiency because its optical band gap is 3.37 eV, and its activity can be increased by many methods such as doping by metals and supporting zeolites [16-17]. The grains of LECA are lightweight, inert chemically, spongy in the

\* Corresponding Author Email: [aref.shokri3@gmail.com](mailto:aref.shokri3@gmail.com)

Table 1. Experimental range and Levels of the variables

Variables	Range and levels		
	-1	0	+1
pH	3	5	7
Cr(VI) (mg L <sup>-1</sup> )	20	40	60
Catalyst Amounts (g L <sup>-1</sup> )	0.25	0.75	1.25

core, neutral pH and insoluble in water [10]. The modified states of LECA were used as suitable adsorbents for the removal of contaminants [18].

To optimize the photo catalytic removal process, it is necessary to study all factors affecting the process. Full factorial design of experiment (FFD) is a suitable method in DOEs, therefore it could reduce the number of experiments and also optimize the process by optimizing all influencing variables. The design could define the effect of each variable on the response and how this result differs with the change in the level of other variables [19].

In this work, the reduction of Cr(VI) by ZnO supported on mineral LECA in aqueous solution was studied. The three factors and three levels of full factorial experimental design was used in photo catalytic removal of Cr(VI). The influence of some operational parameters such as the amount of photo catalyst, initial concentration of Cr(VI) and pH was investigated on the removal of Cr(VI).

## EXPERIMENTAL

### Materials

All materials including Potassium dichromate, Sulfuric acid and Sodium hydroxide, Zinc acetate ( $Zn(CH_3COO)_2 \cdot 2H_2O$ ), and Urea were purchased from the Merck Company (Germany) without further purification. 1, 5-diphenylcarbazide (Merck, purity 98%) was employed as a colorimetric reagent to define the concentration of Cr(VI). Distillate water was used in this study.

### Catalyst preparation

At first the ZnO nanoparticles were synthesized based on the procedure described in our previous work [20], and then the ZnO/LECA was synthesized through co precipitation method. About 2 g of LECA powder was added to 25 ml of zinc oxide solution and then it was stirred for 2 hr. Then 25 ml of urea solution (2.0 M) was added to the mixture at a temperature of 90-95°C and put in a water bath for 6 hr. The mixture was passed through filter paper and the precipitates were dried

at ambient temperature. Sediments were placed in a furnace at 350°C for 3 hr and then the ZnO/LECA was synthesized.

### General procedure

A batch Pyrex reactor with 1000 ml capacity was placed in a wooden box. At the top of the box, three mercury lamps (Philips 15W) were placed as UV light sources. The radiation was performed at 254 nm. These lamps were set up with the same intervals, so the liquid surface was radiated uniformly inside the reactor. A magnetic stirrer agitated the liquid inside the reactor and the air inside the box was ventilated via a fan. For each test (Table 1), 1000 ml of Cr (VI) solution was made at a specified concentration and poured into the reactor.

The Photo catalytic tests were executed by changing the solution pH (3, 5, 7), the amount of catalyst (0.25, 0.75, 1.25 mg/l), and initial Cr (VI) concentration (20, 40, 60 mg/L). Also, the solution pH in the range of 3 to 7 was measured by a pH meter (Schotttitroline TE96) via the addition of NaOH (0.01N) or HCl (0.01N) solutions.

The suspensions of ZnO/LECA were equilibrated in the dark for 30 min. After the equilibration time, the UV lamp was turned on and the samples were withdrawn from the reactor. All tests were performed at a fixed temperature (25°C) for 60 min.

Sampling was performed by a 5 ml syringe every 10 min. The samples were centrifuged at 4,000 rpm for 10 min to separate the catalyst particles. The concentration of Cr(VI) was explored using a spectrophotometer (Perkin Elmer Lamda 25) at a wavelength of 349 nm.

The concentration of Cr(VI) was determined as a function of time as the following (Eq. 1):

$$Cr(VI) \text{ Removal } (\%) = \left( \frac{[Cr(VI)]_0 - [Cr(VI)]}{[Cr(VI)]_0} \right) \times 100 \quad (1)$$

Where  $[Cr(VI)]_0$  and  $[Cr(VI)]$  are the

concentration of Cr (VI) at  $t=0$  and  $t$ , respectively.

#### Full factorial Experimental Design

The photocatalytic efficiency of ZnO/LECA in reducing Cr(VI) to Cr(III) was investigated using FFD. The experiments were designed due to the three variables, including pH, the initial concentration of Cr(VI) and catalyst amount at three levels. The experimental range and levels of variables are shown in Table 1. About 27

experiments related to this factorial design and their experimental conditions have been presented in Table 2. The range of variables was selected based on the preliminary experiments and previous studies.

## RESULTS AND DISCUSSION

### Characterization of the synthesized ZnO/LECA

#### XRD analysis

The XRD test was performed by a D-5000,

Table 2. The three-factor full factorial design pattern and the response function.

Run No.	A: pH	B: Initial Con. of Cr(VI) (mg.L <sup>-1</sup> )	C: Catalyst Amounts (g. L <sup>-1</sup> )	Cr(VI) Removal Efficiency (%)	
				Actual	Predicted
1	3	20	0.25	60.0	59.2259
2	7	20	0.25	49.1	49.0259
3	5	60	0.75	60.2	62.0148
4	7	40	0.25	38.0	37.6481
5	3	60	0.75	50.0	49.4926
6	7	60	0.75	36.0	34.6926
7	7	60	1.25	27.0	27.8815
8	5	40	0.25	74.0	73.9704
9	7	20	1.25	57.3	56.3815
10	7	40	1.25	44.0	44.0370
11	7	20	0.75	62.0	62.9926
12	3	60	1.25	43.0	43.1148
13	5	40	1.25	79.0	79.4259
14	3	40	1.25	55.5	55.0370
15	5	20	0.25	84.6	85.4481
16	7	60	0.25	24.0	24.4259
17	3	20	0.75	72.6	73.0259
18	3	40	0.75	59.3	59.3815
19	5	20	0.75	97.6	96.1815
20	7	40	0.75	48.5	48.8148
21	5	60	0.25	55.8	54.9815
22	3	60	0.25	39.0	39.3926
23	5	40	0.75	82.3	81.9037
24	3	40	0.25	48.0	48.3815
25	5	20	1.25	91.3	91.8704
26	5	60	1.25	58.5	57.5037
27	3	20	1.25	66.5	66.8481

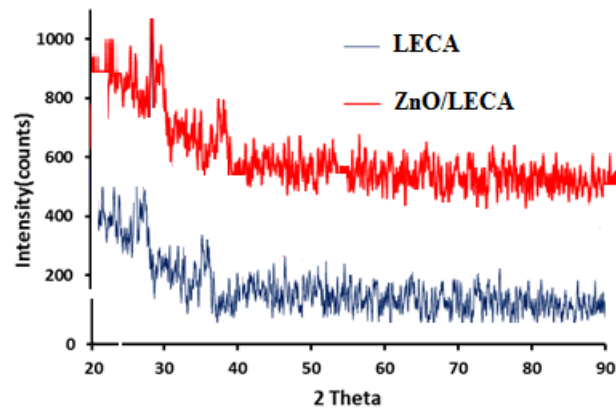
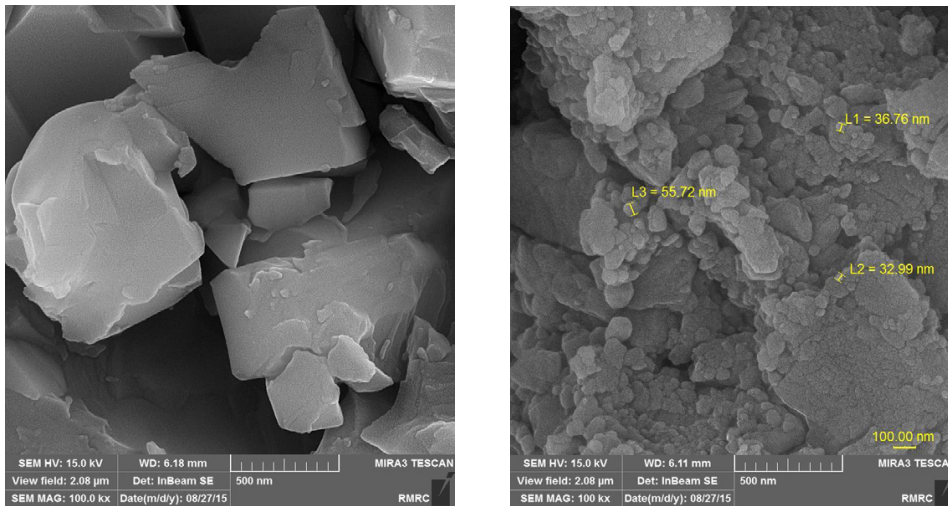


Fig. 1. The XRD pattern of the LECA and ZnO/LECA.



(a) Only ZnO (b) ZnO/LECA

Fig. 2. SEM results of ZnO and ZnO/LECA.

Siemens diffractometer using Cu-K $\alpha$  radiation ( $\lambda=1.5406 \text{ \AA}$ ) coupled with an X-ray tube worked at 40 mA and 30 kV.

Fig. 1 shows the XRD pattern of the synthesized ZnO/LECA. This pattern illustrates that the characteristic peaks in accordance with the LECA were well appeared and it means that the synthesized ZnO/LECA crystals were well-formed [21-22]. The distinct peaks of LECA have occurred well, which indicates that ZnO was stable during the supporting process and it is in agreement with results [23]. The ZnO/LECA particle size was calculated using the Debye-Scherrer equation as the following (Eq.2):

$$d = \frac{0.9\lambda}{\beta \cos \theta} \quad (2)$$

Where K equals 0.9 and  $\beta$  is the Perfect Width at Half- Maximum (FWHM) of the peak,  $\lambda$  is the wavelength of X-ray used  $1.54056 \text{ \AA}$  and  $\theta$  is the Bragg angle. Based on Eq.1, the average particle size of ZnO/LECA was 41.82 nm.

#### FESEM analysis

The field emission scanning electron micrograph (FESEM), Hitachi S-4160 model from Japan, was used for the determination of ZnO/LECA. The SEM images of the LECA with and without supporting ZnO particles were presented in Figs.2. It can be observed that the LECA grains had numbers of pores with different sizes and the surfaces were not fully smooth. The LECA voids were agglomerated with ZnO particles. The result

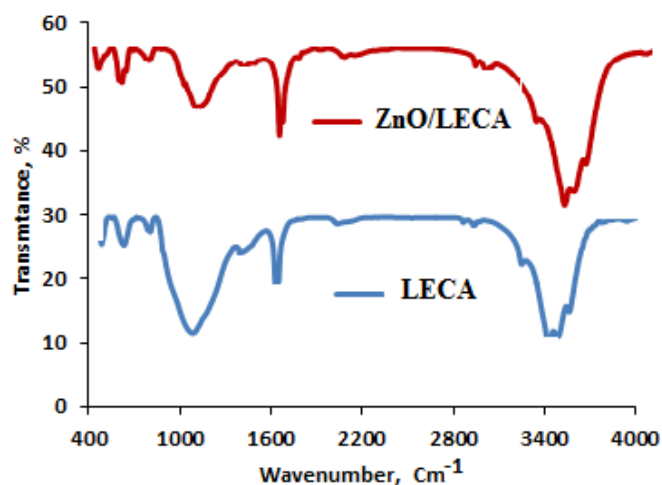


Fig. 3. FTIR analysis of LECA, and ZnO/LECA

Table 3. Analysis of the variance for the quadratic model.

Source	DF	Adj SS	Adj MS	F-value	p-value
Model	18	9097.25	505.40	273.71	0.000
A-pH	2	5036.41	2518.21	1363.79	0.000
B- [Cr(VI)](mg/l)	2	3412.67	1706.33	924.10	0.000
C- [Catalyst](mg/l)	2	512.19	256.09	138.69	0.000
AB	4	107.36	26.84	14.54	0.001
AC	4	10.41	2.6	1.41	0.314
BC	4	18.21	4.55	2.47	0.129
Error	8	14.77	1.85		
Corrected Total	26	9112.02			
R <sup>2</sup>		99.84%			
Adjusted R <sup>2</sup>		99.47%			
Predicted R <sup>2</sup>		98.15%			
S		1.35885			

of our study is in contrast with the findings of Shariefnia et al.[24].

The morphology of the LECA surface showed that it has good structural properties and can be considered catalyst support. In other words, the pores on the surface of this support can perform a suitable condition to support ZnO nanoparticles.

#### FTIR analysis

As it can be seen from Fig. 3, the FTIR spectra of the LECA, ZnO/LECA logged in the range of 400 to 4000. The FTIR spectra of LECA shown that there is a difference in the band intensities in the region of 3500  $\text{cm}^{-1}$ , which originates from the hydroxyl groups on the surface of LECA. The bands detected at 900-1200  $\text{cm}^{-1}$  are related to the Si-O vibrations. The peaks at about 800 to 900  $\text{cm}^{-1}$  match with the Si-O-Al, Al-OH-Al and Al-OH-Zn groups. The observed peak at 1700  $\text{cm}^{-1}$  is related to the physical

adsorbed water. For ZnO/LECA spectra, the band about 600  $\text{cm}^{-1}$  relating to the Zn-O metal oxide bond and the peaks at about 1500  $\text{cm}^{-1}$  relate to the C-O bonds. The band at 1600  $\text{cm}^{-1}$  is allocated to O-H bending vibrations. The peaks at about 1000  $\text{cm}^{-1}$  match with the Al-OH-Zn groups. It was clear that when ZnO is settled over LECA, there is a dissimilarity in the intensity of peak between LECA and ZnO/LECA, signifying that ZnO particles have been efficiently covered on the surface of LECA.

#### Experimental Design and Statistical Analysis

The experimental design matrix and the actual and predicted values of the response were presented in Table 2. It was clear that a good uniformity exists between the predicted values by the model and the actual values in the experiments.

The analysis of variance is shown in Table 3. The model F-value of 273.71 proposes that

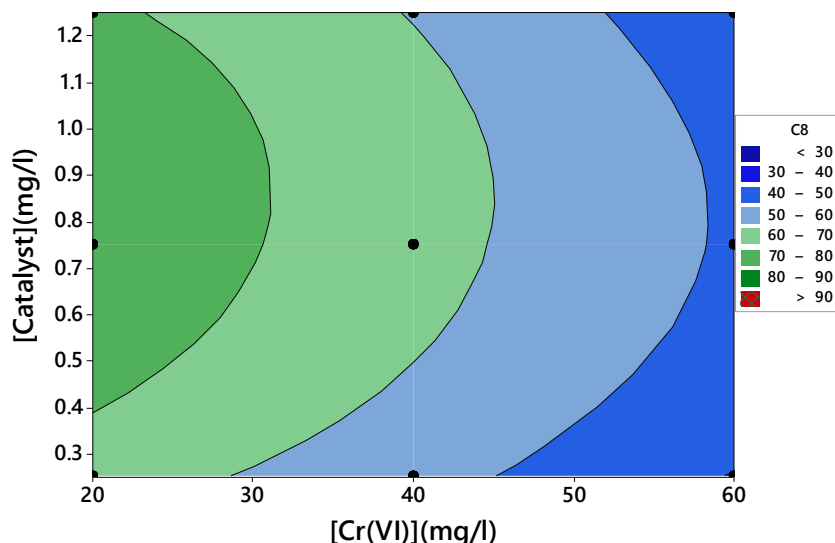


Fig. 4. Effect of initial Cr(VI) and catalyst concentration.

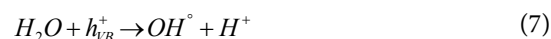
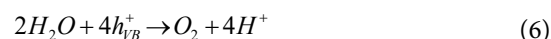
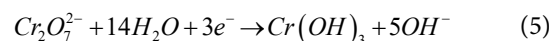
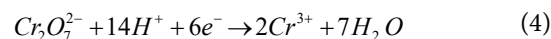
the model is significant. Note that there exists only a 0.00% chance that this large F-value could arise due to noise [25-26]. The model terms are called significant part, where the corresponding probability values (p-values) are lower than 0.0500. The p-values higher than 0.1000 denotes that the model terms are insignificant.

To predict the response for known levels of each parameter, the final equation can be applied in terms of code parameters. Accordingly, the high and low levels of the parameters are coded as +1 and -1, respectively. The coded equation helps detect the relative effect of the parameters on the response by comparing the parameter coefficients. As given in the coded equation, the coefficients of A, C A<sup>2</sup>, B<sup>2</sup>, and C<sup>2</sup> are greater than the other factors/interactions, which depict that these factors have a higher influence on the response value. The equation in terms of actual factors can predict the response, where the levels should be specified in the original units for each factor. The slight difference between the Predicted R<sup>2</sup> (0.9815) and Adjusted R<sup>2</sup> (0.9947) is less than 0.2, indicating that there is a reasonable agreement between them.

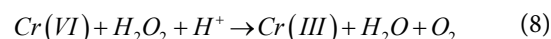
*Photo catalytic mechanism*

Under UV irradiation, the pairs of electron-holes produced at the surface of ZnO/LECA(Eq.3). After the separation of the electron-hole pairs, the Cr(VI) was reduced to Cr(III) by electrons(Eq.4), and the holes might lead to the production of O<sub>2</sub>

in the absence of organics[27]. The reduction of Cr(VI) to Cr(III) by a photo catalytic process can be proposed through the following mechanism:



The reduction reagents are significant to remove Cr(VI) as an oxidative contaminant. The reduction of Cr(VI) with hydrogen peroxide results in Cr(III) (Eq.8) [28-29].



*Effect of initial Cr(VI) concentration*

As shown in Fig. 4, the removal efficiency of Cr (VI) was decreased with increasing its initial concentration. The absorption of light beams in the solution was increased with an increase in the concentrations of potassium dichromate. Therefore, the light that can reach the photo catalyst surface is reduced and the efficiency of the process was decreased [30]. In another word, the absorbance of the solution was enhanced to increase in the



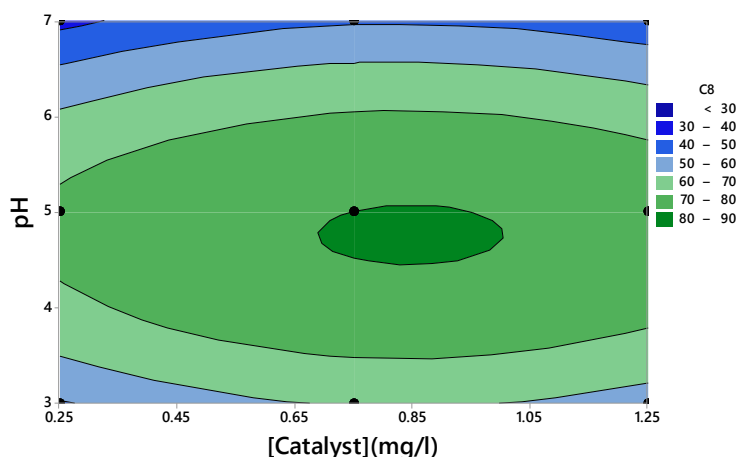


Fig. 5. Effect of pH and catalyst concentration.

concentration of  $K_2Cr_2O_7$  and a higher portion of the UV radiation is diverted before it touches the surface of the ZnO/LECA, thus falling the conversion of Cr (VI). Similar phenomena were reported formerly by Preethia et al., [31]. It should be noted that, for a fixed dosage of catalysts, the entire existing active sites were restricted, therefore leading to a decline in reduction of Cr(VI) with its increased initial concentration from 20 to 60 mg/L. Also, the extent of available electron-hole pairs was restricted to get a high reduction of Cr(VI) at its increased initial concentration. Based on the experimental results, 20 mg/L was set as optimum Cr(VI) concentration.

#### Effect of catalyst concentration

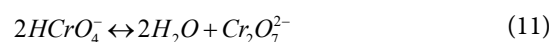
By increasing the amounts of ZnO/LECA photocatalyst, the removal of Cr(VI) was increased because under UV radiation, the formation of electron-hole pairs in the structure of the catalyst was increased. Increasing the amount of catalyst improves the capture of UV radiation by nanoparticles and the percent of reduction of Cr(VI) rises [32]. It is clear from Fig.5 that, as the dosage increases from 0.25 to 0.75 mg/l, the reduction efficiency of Cr(VI) was enhanced due to the increase in the active sites and the number of photons adsorbed and subsequently increased in the adsorption of Cr(VI) and reduction to Cr(III). After 0.75 mg/l of catalytic dosage, the proportion of photo-reduction has not been improved considerably and this may be due to the fact that this dosage level may be sufficient for reducing the Cr(VI) concentration tested.

#### Effect of pH

The photocatalytic removal of Cr(VI) was higher in acidic pH since the removal reaction in acidic solution was performed well. Moreover, electrons in the conduction band ( $e_{CB}^-$ ) of catalyst area can reduce molecular oxygen to superoxide anion [33]. Therefore, the pair of hydrogen peroxide and oxygen is formed in an acidic solution and Cr(VI) reduces by Hydrogen peroxide.

High removal of Cr(VI) was occurred at lower pH, because of an enhanced potential difference between the conduction band of Cr(VI)/Cr(III) and ZnO/LECA as well as the anionic-type adsorption of Cr(VI) onto the catalyst surface. As previously discussed by other researchers, the potential difference between the conduction band of catalyst and the Cr(VI) is a thermodynamic driving force for the reduction of Cr(VI) [34].

The influence of pH on the photocatalytic reduction of Cr (VI) is different from the results of adsorption studies. Perhaps, the removal of Cr(VI) in basic and acidic conditions happens through the following reactions [35]:



But, the photocatalytic reduction of Cr(VI) to Cr(III) creates hydroxyls in alkaline solution and consumes protons in acidic solution. So the reduction percentage of Cr(VI) to Cr(III) drops

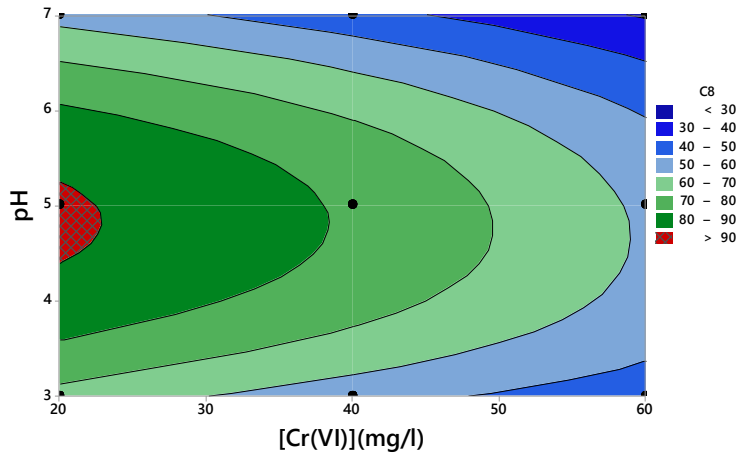


Fig. 6. Effect of pH and initial Cr(VI) concentration.

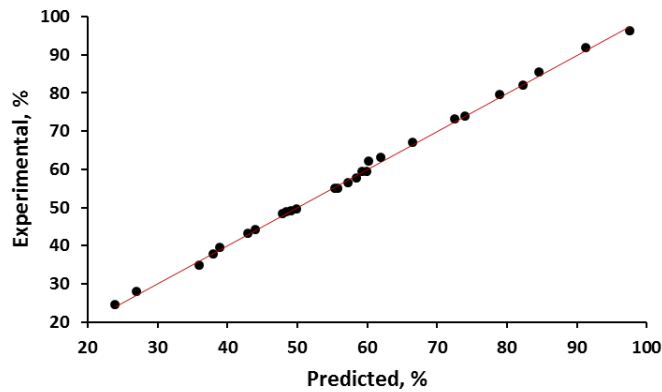
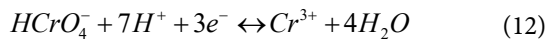


Fig. 7 Comparison between experimental results and predicted values in FFD.

with increasing pH. As it is possible to consider by Eq. (12), this species needs three moles of electrons and seven moles of protons to reduce one mole of hexavalent chromium



An appropriate pH range for the reduction of Cr(VI) using ZnO was between 4 and 8, since the pH values of groundwater and soil were generally between 5 and 9 [35], so ZnO/LECA may be employed in reduction of Cr(VI) polluted aqueous solutions in a broader range of pH. The catalyst dissolves in acidic and basic solutions and high pH is damaging reduction reagents.

The comparison of experimental results and the predicted amounts by the FFD are shown in Fig. 6. The correlation coefficient ( $R^2$ ) is a quantitative

standard for calculating the correlation between the predicted values and the experimental data. The value of  $R^2 = 0.99$  shows the good agreement and the relationship between the experimental and the predicted data by the full factorial.

The difference between the predicted and experimental response values is called as the residual values, which was calculated to examine the validity of the model. The dispersion of the residual values was shown in Fig. 7. The linear nature of the plot showed that the model is considered correct.

## CONCLUSIONS

In this study, the ZnO was supported on LECA as a synthesized nano photocatalyst and it was used to reduce Cr(VI) to Cr(III) in an aqueous solution through a batch photo reactor. The SEM, FTIR and XRD patterns were used for the characterization



of ZnO/LECA. The FFD was used for statistical analysis of data. The influence of catalyst amounts, pH, and initial concentration of Cr (VI) were investigated on the reduction percent of Cr (VI) to Cr (III). High removal of Cr(VI) was occurred at lower pH, because of an enhanced potential difference between the conduction band of Cr(VI)/Cr(III) and ZnO/LECA as well as the anionic-type adsorption of Cr(VI) onto the catalyst surface. The optimal conditions were obtained at 0.75 g/l of photo catalyst, pH at 5 and concentrations of Cr(VI) at 20 mg/l. The experimental and predicted reduction efficiency by FFD at optimal conditions was 97.6 and 96.18%, respectively.

#### ACKNOWLEDGEMENTS

The project is funded by the Jundi-shapur Research Center in Dezful, Iran.

#### CONFLICT OF INTEREST

The authors declare that there is no conflict of interest regarding the publication of this manuscript.

#### REFERENCES

1. S Nezar, Y Cherifi, A Barras, A Addad, E Dogheche, N Saoula, N Aïcha Laoufi, P Roussel, S Szunerits, R Boukherroub. Arab. J. Chem. 12:215(2019). <https://doi.org/10.1016/j.arabjc.2018.01.002>
2. Q Meng, Y Zhou, G Chen, Y Hu, C Lv, L Qiang, W Xing. Chem. Eng J. 334:334(2018). <https://doi.org/10.1016/j.cej.2017.07.134>
3. E Liu, Y Du, X Bai, J Fan, X Hu. Arab J Chem. 13:3836(2020). <https://doi.org/10.1016/j.arabjc.2019.02.001>
4. K Wang, P Chen, W Nie, Y Xu, Y Zhou. Chem Eng J. 359:1205(2019). <https://doi.org/10.1016/j.cej.2018.11.057>
5. R Yin, L Ling, Y Xiang, Y Yang, AD Bokare, C Shang. Sep. Purif. Technol. 190:53(2018). <https://doi.org/10.1016/j.seppur.2017.08.042>
6. M Li, Q Hu, H Shan, W Yu, Z X Xu. Chemosphere, 263:128250(2021). <https://doi.org/10.1016/j.chemosphere.2020.128250>
7. S Sadrieh, E Mohsen, G G Bakeri. Synthetic Metals, 267:116470(2020). <https://doi.org/10.1016/j.synthmet.2020.116470>
8. X Wang, L Li, J Meng, P Xia, Y Yang, Y Guo. Appl. Surf. Sci. 506:144181(2020). <https://doi.org/10.1016/j.apusc.2019.144181>
9. R Li, D Hu, K Hu, H Deng, M Zhang, A Wang, R Qiu, K Yan. Sci. Total Environ. 704:135284(2020) <https://doi.org/10.1016/j.scitotenv.2019.135284>
10. L Guo, KL Zhang, H Shen, C Wang, Q Zhao, D Wang, F Fu, Y Liang. Chem Eng J. 370:1522(2019). <https://doi.org/10.1016/j.cej.2019.04.037>
11. Y Xu, D Wang, M Xie, L Jing, Y Huang, L Huang, H Xu, H Li, J Xie. Mater. Res. Bull. 112:226(2019). <https://doi.org/10.1016/j.materresbull.2018.12.017>
12. P Karthik, B Neppolian. J. Environ. Chem. Eng. 6: 3664(2018). <https://doi.org/10.1016/j.jece.2017.05.028>
13. V Ramya, D Murugan, C Lajapathirai, A Sivasamy. J. Environ. Chem. Eng. 6: 7327(2018). <https://doi.org/10.1016/j.jece.2018.08.055>
14. X Zhao, S Huang, Y Liu, Q Liu, Y Zhang. J Hazard Mater. 353:466(2018). <https://doi.org/10.1016/j.jhazmat.2018.04.005>
15. XF Wu, H Li, JZ Su, JR Zhang, YM Feng, YN Jia, LS Sun, WG Zhang, M Zhang, CY Zhang. Appl Surf Sci. 473:992(2019). <https://doi.org/10.1016/j.apusc.2018.12.219>
16. N Seifvand, E Kowsari. Appl. Catal. B-Environ. 2017; 206:184-93. <https://doi.org/10.1016/j.apcatb.2017.01.024>
17. A Shokri, M Salimi, T Abmatin. Fresen Environ Bull 26 (2 A), 1560-1565.
18. Z Wu, CL Peacock, B Lanson, H Yin, L Zheng, Z Chen, W Tan, G Qiu, F Liu, X Feng. T. Geochim Cosmochim Acta. 246:21(2019). <https://doi.org/10.1021/es2013038>
19. A Shokri. Int. J. Ind. Chem. 9:295(2018). <https://doi.org/10.1007/s40090-018-0159-y>
20. A Shokri, R Hekmatshoar, A Yari. J. Nanoanalysis(2020). <https://doi.org/10.22034/jna.2020.1898029.1205>
21. M Bordbar, S Forghani-pilerood, A Yeganeh-Faal. Iran J Catal. 6:415(2016).
22. S Aghdasi, M Shokri. Iran J Catal. 6:481(2016).
23. SV Balakhonov, BR Churagulov, EA Gudilin. J Surf Invest. 2008; 2:152-5.
24. H Moradi, S Sharifnia, F Rahimpour. Mate. Chem. Phys. 158:38 (2015). <https://doi.org/10.1016/j.matchemphys.2015.03.031>
25. A Shokri. Int. J. Environ. Anal. Chem., 1(2020)15. <https://doi.org/10.1080/03067319.2020.1791328>
26. A Shokri. Desal Water Treat. 115: 281(2018).<https://doi.org/10.5004/dwt.2018.22451>
27. K Kabra, R Chaudhary, RL Sawhney. Ind Eng Chem Res 43:7683(2004). <https://doi.org/10.1021/ie0498551>
28. X Deng, YChen, J Wen, Y Xu, J Zhu, Z Bian. Science Bulletin,65:105(2020). <https://doi.org/10.1016/j.scib.2019.10.020>
29. Y Wang, S Bao, Y Liu, W Yang, Y Yu, M Feng, K Li. Appl. Surf. Sci. 510:155495(2020). <https://doi.org/10.1016/j.apusc.2020.145495>
30. S Chakrabarti, B Chaudhuri, S Bhattacharjee, AK Ray, BK Dutta. Chem Eng J. 153(2009)86. <https://doi.org/10.1016/j.cej.2009.06.021>
31. J Preethia, M H Farzana, S Meenakshi. Int J Biol Macromol. 104: 1783(2017). doi: 10.1016/j.ijbiomac.2017.02.082.
32. YG Liu, XJ Hu, H Wang, AW Chen, SM Liu, YM Guo, YHe, X Hu, J Li, SH Liu, YQ Wang, L Zhou. Chem. Eng. J. 226:131 (2013). <https://doi.org/10.1016/j.cej.2013.04.048>
33. Z Jin, YX Zhang, FL Meng, Y Jia, T Luo, XY Yu, J Wang, JH Liu, XJ Huang. J Hazard. Mater. 276:400 (2014). <https://doi.org/10.1016/j.jhazmat.2014.05.059>
34. X Liuyang, H Yang, S Huang, Y Zhang, S Xia. J. Environ. Chem. Eng., 8: 104474 (2020). <https://doi.org/10.1016/j.jece.2020.104474>
35. A Asadi, MH Deghani, N Rastkari, S Nasseri, AH Mahvi. Environ. Protec. Eng. 38: 5(2012). <http://dx.doi.org/10.5277/EPE120401>